

Synthesis and Self-Assembly of Amphiphilic Polymeric Microparticles

Dhananjay Dendukuri, T. Alan Hatton, and Patrick S. Doyle*

Department of Chemical Engineering, Massachusetts Institute of Technology, 77 Massachusetts Avenue, Cambridge, Massachusetts 02139

Received August 25, 2006. In Final Form: October 19, 2006

We report the synthesis and self-assembly of amphiphilic, nonspherical, polymeric microparticles. Wedge-shaped particles bearing segregated hydrophilic and hydrophobic sections were synthesized in a microfluidic channel by polymerizing across laminar coflowing streams of hydrophilic and hydrophobic polymers using continuous flow lithography (CFL). Particle monodispersity was characterized by measuring both the size of the particles formed and the extent of amphiphilicity. The coefficient of variation (COV) was found to be less than 2.5% in all measured dimensions. Particle structure was further characterized by measuring the curvature of the interface between the sections and the extent of cross-linking using FTIR spectroscopy. The amphiphilic particles were allowed to self-assemble in water or at water–oil interfaces. In water, the geometry of the particles enabled the formation of micelle-like structures, while in emulsions, the particles migrated to the oil–water interface and oriented themselves to minimize their surface energy.

1. Introduction

Polymeric microparticles and colloids are essential for both fundamental studies and a wide variety of applications ranging from drug delivery to paints and catalysis. While spherical polymeric particles are ubiquitous, complex particles with nonspherical shapes and chemical anisotropy offer several unique advantages relative to their spherical counterparts. In particular, their ability to assemble into a wide range of crystal structures unavailable to spheres¹ and their anisotropy-driven response to interfacial forces and external fields could lead to a variety of technologically important applications. To cite only a few examples, dipolar particles are already being used as the components of e-paper,² specifically designed nonspherical particles may be used as the building blocks of photonic crystals with complete band gap,¹ and amphiphilic particles can be used as extremely effective particle surfactants.³ In all these applications, the precise tuning of particle morphology and chemistry is imperative. Further, in the bottom-up approach envisioned to build materials and devices of the future efficiently,⁴ one would like to preprogram the structure or bulk properties of supraparticular assemblies through precisely designed building blocks. The specific interactions caused by the geometrical anisotropy and chemical inhomogeneity of the building blocks are then vital to their assembly and the macroscopic properties of the superstructures formed. A particle synthesis method that enables the tuning of both geometric parameters, e.g., shape and size, as well as chemical inhomogeneity, is thus highly desirable.

Microfluidics has recently emerged as a promising route to the synthesis of such complex materials.^{2,5–13} It offers the

advantage of continuous processing in addition to fine temporal and spatial control, enabling the formation of spherical particles,⁵ nonspherical bubbles,¹² colloidal particle assemblies in droplets,^{6,11} solid particles,^{2,8–10,13} and fibers.⁷ In microfluidic devices, solid nonspherical polymeric particles have been synthesized by polymerizing highly reactive polymeric precursors that cross-link on exposure to UV light or heat.^{7–10,13} In two-phase microfluidic flows, droplets of polymer precursors have been confined geometrically to form nonspherical shapes,^{8,9} while in one-phase flows, particle shape has been conveniently defined by using a photomask.¹³ By using specific polymer chemistries or by loading the polymeric precursors used with liquid crystals, magnetic materials, quantum dots, dyes, and so forth, one can synthesize particles that bear both complex shapes and a specific chemical or physical functionality. This enables the creation of chemically diverse but homogeneous sets of nonspherical particles like ellipsoids, disks, and rods,^{7–9} and indeed any extruded 2-D shape.¹³ However, it is much more challenging to synthesize chemically inhomogeneous polymeric particles with nonspherical shapes. Some groups have reported the microfluidic synthesis of spherical particles with multiple chemistries,² or barcoded strips¹⁴ that bear different chemistries. Others have used electrical^{15,16} or surface-force driven¹⁷ microdroplet manipulation techniques to synthesize topologically complex spherical droplets. A variety of other nonmicrofluidic methods¹⁸ have also been developed to synthesize Janus particles. Most methods involve

* E-mail: pdoyle@mit.edu.

- (1) Lu, Y.; Yin, Y.; Xia, Y. *Adv. Mater.* **2001**, *13*, 415–420.
- (2) Nisisako, T.; Torii, T.; Takahashi, T.; Takizawa, Y. *Adv. Mater.* **2006**, *18*, 1152–1156.
- (3) Casagrande, C.; Fabre, P.; Raphael, E.; Veyssie, M. *Europhys. Lett.* **1989**, *9*, 251–255.
- (4) Glotzer, S. C. *Science* **2004**, *306*, 419–420.
- (5) Nisisako, T.; Torii, T.; Higuchi, T. *Chem. Eng. J.* **2004**, *101*, 23–29.
- (6) Yi, G.-R.; Thorsen, T.; Manoharan, V. N.; Hwang, M.-J.; Jeon, S.-J.; Pine, D. J.; Quake, S. R.; Yang, S.-M. *Adv. Mater.* **2003**, *15*, 1300–1304.
- (7) Jeong, W.; Kim, J.; Kim, S.; Lee, S.; Mensing, G.; Beebe, D. J. *Lab Chip* **2004**, *4*, 576–580.
- (8) Dendukuri, D.; Tsoi, K.; Hatton, T. A.; Doyle, P. S. *Langmuir* **2005**, *21*, 2113–2116.

- (9) Xu, S.; Nie, Z.; Seo, M.; Lewis, P.; Kumacheva, E.; Stone, H. A.; Garstecki, P.; Weibel, D. B.; Gitlin, I.; Whitesides, G. M. *Angew. Chem., Int. Ed.* **2005**, *44*, 724–728.
- (10) Nie, Z.; Xu, S.; Seo, M.; Lewis, P. C.; Kumacheva, E. *J. Am. Chem. Soc.* **2005**, *127*, 8058–8063.
- (11) Subramaniam, A. B.; Abkarian, M.; Stone, H. A. *Nat. Mater.* **2005**, *4*, 553–556.
- (12) Subramaniam, A. B.; Abkarian, M.; Mahadevan, L.; Stone, H. A. *Nature (London)* **2005**, *438*, 930.
- (13) Dendukuri, D.; Pregibon, D. C.; Collins, J.; Hatton, T. A.; Doyle, P. S. *Nat. Mater.* **2006**, *5*, 365–369.
- (14) Kim, S.; Oh, H.; Baek, J. Y.; Kim, H.; Kim, W.; Lee, S. *Lab Chip* **2005**, *5*, 1168–1172.
- (15) Millman, J. R.; Bhatt, K. H.; Prevo, B. G.; Velev, O. D. *Nat. Mater.* **2005**, *4*, 98–102.
- (16) Roh, K.-H.; Martin, D. C.; Lahann, J. *Nat. Mater.* **2005**, *4*, 759–763.
- (17) Fialkowski, M.; Bitner, A.; Grzybowski, B. A. *Nat. Mater.* **2005**, *4*, 93–97.
- (18) Perro, A.; Reculusa, S.; Ravaine, S.; Bourgeat-Lami, E.; Duguet, E. *J. Mater. Chem.* **2005**, *15*, 3745–3760.

the selective surface modification of spherical precursor particles. While nonspherical shapes have been synthesized using multilayer photolithography¹⁹ and manual fabrication,²⁰ it is difficult to use these methods to synthesize particles with more than two chemistries or finely tune the extent of each chemistry in the particle. There is therefore a distinct need for a single-step particle synthesis method to form different nonspherical shapes with tunable anisotropy and with the ability to incorporate more than two chemical functionalities.

We have recently proposed a method to synthesize such complex particles using a technique called continuous flow lithography (CFL).¹³ Using CFL, mask-defined shapes can be polymerized into a flowing stream of monomer using short pulses of UV light (typically <0.1 s in duration). This enables the process to be continuous, increasing its throughput, and also allows for particle formation across multiple laminar coflowing streams, enabling the formation of particles with tunable chemical anisotropy. Previously, we demonstrated that CFL can be used to fabricate “bar-coded” particles by polymerizing across miscible, chemically similar coflowing streams. In this case, the interface between the different regions in a particle is not sharp due to molecular diffusion. Furthermore, the miscible nature of the fluids means that the different regions of the particle will typically have similar surface energies. In this paper, we use CFL to synthesize particles with specific shapes that bear spatially segregated chemistries with contrasting properties and different surface energies. To accomplish this, we use parallel streams of immiscible polymer coflowing through a microfluidic device. The use of immiscible fluids in microfluidic devices has been explored extensively²¹ to study, for example, drug partitioning behavior,²² to achieve tunable liquid microlenses,²³ to perform interfacial reactions,²⁴ or to accomplish separations.²⁵ Others have probed the experimental phase space of device operation using immiscible fluids to determine conditions when different regimes such as droplet breakoff^{26,27} and parallel coflow^{28–30} are observed. In our study, coflowing immiscible photopolymeric materials are used to synthesize particles with a sharp interface separating hydrophilic and hydrophobic sections. After synthesizing the particles, we exploit their “amphiphilic” nature by allowing them to self-assemble in water and at oil–water interfaces. Like their molecular analogs, the particles assemble differently in water, o/w, or w/o emulsions in order to minimize their surface energy.

Amphiphilic molecules are often represented by objects in the spectrum of shapes between a cone and a cylinder, where the body of the object represents the hydrophobic tail and the hydrophilic head is represented by one of the circular faces.³¹

This spectrum of shapes is used to show the effect of geometry on packing. Changing the geometry of the molecules results in different aggregated structures such as micelles, bilayers, and reversed micelles being formed. The two-dimensional analogs of such objects are wedge shapes that fall in the spectrum between triangles and rectangles. We therefore chose to synthesize amphiphilic wedge-shaped particles—both to illustrate the power of CFL to synthesize any extruded 2-D shape and to allow for geometry-induced aggregation later in our study. Analogous to the molecular scale, amphiphilic particles synthesized in our study have a hydrophilic head and a hydrophobic tail, whose relative proportions can be easily changed.

2. Experimental Methods

Materials. The hydrophobic phase consisted of a 5% (v/v) solution of Darocur 1173 (Sigma Aldrich) initiator in tri(methylol propane) triacrylate (TMPTA, Polysciences). The hydrophilic phase consisted of 5% (v/v) solutions of Darocur 1173 (Sigma Aldrich) initiator in a 65% aqueous solution of poly(ethylene glycol) (600) diacrylate (PEG-DA, Sigma Aldrich). Since TMPTA is insoluble in water, the two phases were immiscible. PEG-DA and TMPTA are reported by the manufacturer to have viscosities of 90 cPs and 106 cPs at 25 °C.

Microfluidic Devices. Devices were fabricated by pouring polydimethylsiloxane (PDMS, Sylgard 184, Dow Corning) on a silicon wafer containing positive-relief channels patterned in SU-8 photoresist (Microchem). The devices were Y-shaped rectangular channels of width 200 or 300 μm and height 30 μm . These devices were placed on glass slides spin-coated with PDMS to ensure that the oligomer was exposed only to PDMS surfaces. Devices were mounted on an inverted microscope (Axiovert 200, Zeiss), and the formation of the microparticles was visualized using a CCD camera (KPM1A, Hitachi). Images were captured and processed using NIH Image software or a Nikon D200 camera and Nikon Capture software.

Photopolymerization Setup. Photomasks were designed in AUTOCAD 2005 and printed using a high-resolution printer at CAD Art Services (Poway, CA). The mask was then inserted into the field-stop of the microscope. A 100 W HBO mercury lamp served as the source of UV light. A filter set that provides wide UV excitation (11000v2: UV, Chroma) was used to select light of the desired wavelength, and a VS25 shutter system (Uniblitz) driven by a computer controlled VMM–D1 shutter driver provided specified pulses of UV light. Oligomer solutions were driven through the microfluidic device using a KDS 100 syringe pump (KD Scientific). Particles were formed across the interface of the two streams after aligning the mask shapes to be parallel to the interface. Typical exposure times used were 0.03–0.05 s, and flow velocities used varied between 100–300 $\mu\text{m/s}$. All particles shown in this study were made using exposure times of 0.03 s. A reservoir was cut in the PDMS to collect the particles.

Particle Characterization and Emulsion Formation. The sizes of the particles were estimated as they were being formed by capturing images of the flowing particles using low camera exposure times (1/10 000 s). Statistics were estimated on 100 consecutive particles formed at an exposure time of 0.03 s. Conversion of double bonds was estimated using FTIR spectroscopy performed on a Nicolet spectrometer (Thermo Corp.), by measuring the decrease in terminal C=C stretch at 1635 cm^{-1} in a thin film of cross-linked polymer.³² To perform FTIR, individual samples of either the hydrophilic or the hydrophobic monomer were prepared by loading the respective oligomer into a channel with the same dimensions as the device used and then given exposure doses of 0.03 s (same as the formed particles) and 120 s (fully cross-linked). Strips of polymer film were formed that were used for FTIR measurements. Contact angle measurements were performed using the sessile drop method and a DSA 10 tensiometer (Kruss). Advancing contact angle measurements were made on a drop of the required polymer placed on a clean PDMS surface.

(19) Brown, A. B. D.; Smith, C. G.; Rennie, A. R. *Phys. Rev. E* **2000**, *62*, 951–960.

(20) Bowden, N.; Terfort, A.; Carbeck, J.; Whitesides, G. M. *Science* **1997**, *276*, 233–235.

(21) Atencia, J.; Beebe, D. J. *Nature (London)* **2005**, *437*, 648–655.

(22) Surmeian, M.; Slyadnev, M. N.; Hisamoto, H.; Hibara, A.; Uchiyama, K.; Kitamori, T. *Anal. Chem.* **2002**, *74*, 2014–2020.

(23) Dong, L.; Agarwal, A.; Beebe, D.; Jiang, H. *Nature (London)* **2006**, *442*, 551–554.

(24) Zhao, B.; Viernes, N. O. L.; Moore, J. S.; Beebe, D. J. *Anal. Chem.* **2002**, *74*, 5284–5285.

(25) Zabow, G.; F. Assi, R. J.; Prentiss, M. *Appl. Phys. Lett.* **2002**, *80*, 1483–1485.

(26) Thorsen, T.; Roberts, R. W.; Arnold, F. H.; Quake, S. R. *Phys. Rev. Lett.* **2001**, *86*, 4163–4166.

(27) Anna, S. L.; Bontoux, N.; Stone, H. A. *Appl. Phys. Lett.* **2003**, *82*, 364–366.

(28) Dreyfus, R.; Tabeling, P.; Willaime, H. *Phys. Rev. Lett.* **2004**, *90*, 144505.

(29) Engl, W.; Ohata, K.; Guillot, P.; Colin, A.; Panizza, P. *Phys. Rev. Lett.* **2006**, *96*, 134505.

(30) Guillot, P.; Colin, A. *Phys. Rev. E* **2005**, *72*, 066301.

(31) Israelachvili, J. N. *Intermolecular and Surface Forces*, 1st ed.; Academic Press: Orlando, 1985.

(32) Mellott, M. B.; Searcy, K.; Pishko, M. V. *Biomaterials* **2001**, *22*, 929–941.

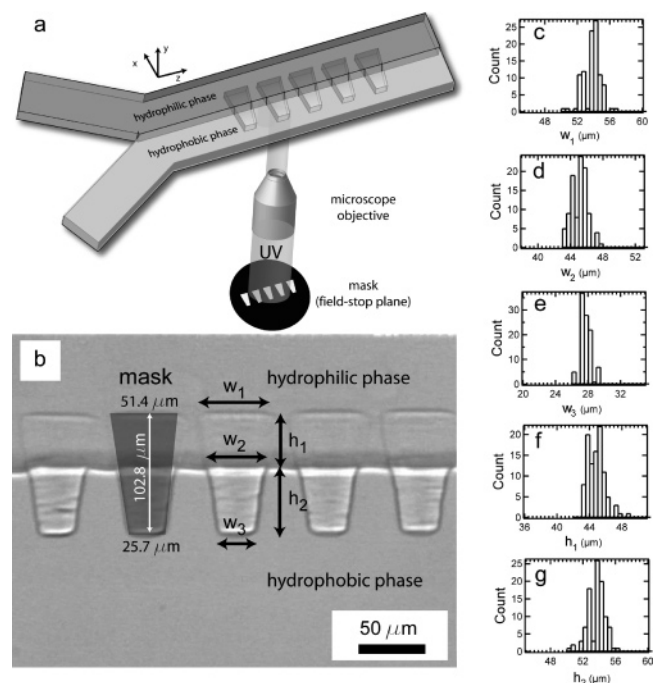


Figure 1. Synthesis of biphasic particles containing hydrophilic and hydrophobic chemistries. (a) Schematic depicting the formation of biphasic particles. Mask-defined wedge shapes are polymerized, five at a time, across two parallel coflowing streams containing hydrophilic and hydrophobic chemistries using continuous flow lithography. (b) Bright field image of five particles simultaneously being polymerized across coflowing immiscible streams—one containing an aqueous solution of a hydrophilic oligomer (PEG-DA) and the other containing a hydrophobic oligomer (TMPTA). The expected dimensions of the particle are overlaid on the second particle from the left. The dimensions of interest are labeled on the third particle from the left. The dimensions of interest are labeled on the third particle from the left. (c–g) Histograms showing the distribution of sizes in the dimensions of interest. These were measured as the particles were being made in the device. The mean values obtained are $w_1 = 53.7 \mu\text{m}$, $w_2 = 45.1 \mu\text{m}$, $w_3 = 27.7 \mu\text{m}$, $h_1 = 44.8 \mu\text{m}$, and $h_2 = 53.6 \mu\text{m}$. In all five dimensions, the COV is less than 2.5%. In addition, the thickness of the particles (in the y-dimension) is measured to be 25 μm .

To make w/o type emulsions, 20 μL of toluene was added to 10 μL of a water-in-monomer emulsion, containing the particles isolated from the reservoir, and then agitated using a vortex mixer. Both monomers are soluble in toluene, resulting in the formation of water-in-toluene droplets. To make o/w type emulsions, 5 μL of a water-in-monomer emulsion, containing the particles isolated from the reservoir, along with 5 μL of toluene was added to 20 μL of DI water and then agitated using a vortex mixer. This resulted in the formation of toluene-in-water droplets. 20 μL of either emulsion is then sandwiched between two PDMS-coated glass slides in order to create two-dimensional structures for observation on the microscope.

3. Results and Discussion

An all-PDMS, Y-shaped, microfluidic device containing two ports, one to introduce each phase, is used in the synthesis of the particles (Figure 1a). The device is placed on a movable microscope stage, and UV light is provided from a mercury lamp attached to the microscope. A hydrophilic phase consisting of an aqueous solution of poly(ethylene glycol) diacrylate (PEG-DA) and a hydrophobic phase consisting of tri(methylolpropane) triacrylate (TMPTA) flow parallel to each other through the rectangular channel, with stream widths controlled by their relative flow rates and viscosities. The flow rates for the two streams are constrained to be in a regime where parallel coflow is observed.³⁰

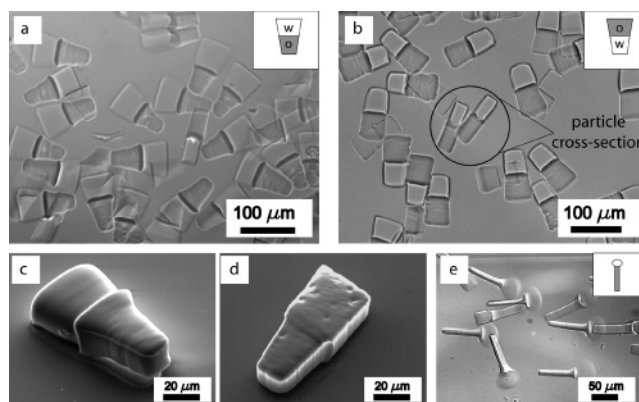


Figure 2. Biphasic particles synthesized using CFL. The inset in (a), (b), and (e) shows the type of particle in each figure. The hydrophilic head is represented in white and indicated by the letter w, while the hydrophobic tail is represented in gray and indicated by the letter o. (a) Differential interference contrast (DIC) images of particles with a large hydrophilic head and a smaller hydrophobic tail in ethanol. The particles were made at exposure times of 0.03 s and flow rates of 0.1 $\mu\text{L}/\text{min}$ for each stream, collected in a reservoir and washed in ethanol. The ethanol swells the large hydrophilic head, resulting in a slight distortion from the original shape. (b) DIC images of particles with a small hydrophilic head and a larger hydrophobic tail in ethanol. Particles were made at exposure times of 0.03 s and flow rates of 0.05 $\mu\text{L}/\text{min}$ for each stream. The ethanol now swells the small hydrophilic head. (c) SEM image of one of the particles in (a). The hydrophilic head has shrunk on drying. (d) SEM image of one of the particles in (b). The hydrophilic portion has shrunk on drying. (e) DIC images of ball-and-stick model biphasic particles with a hydrophilic disk-shaped head and a long hydrophobic tail.

As illustrated in Figure 1a,b, wedge-shaped particles are polymerized, five at a time, across the coflowing streams using projection lithography and a 20 \times microscope objective. Copolymerization of the two acrylates used leads to a chemical linkage of the hydrophilic and hydrophobic sections at the interface, lending stability to the particles formed. The particles synthesized are approximately $1/8$ of their mask size and are able to form and flow continuously because of the oxygen-induced inhibition³³ of polymerization at PDMS surfaces. During the polymerization process, oxygen diffusing in through the PDMS reacts with the initiator species, converting them to chain-terminating peroxide radicals. This results in the formation of a thin, uncrosslinked, lubricating layer of oligomer near the PDMS walls that enables the particles to flow.¹³ A reservoir used to collect the particles is positioned immediately downstream of the polymerization zone so that the particles formed exit the microchannel and do not alter the flow profile upstream. In our setup, the proportions of the hydrophilic and hydrophobic sections could be conveniently altered by moving the microscope stage, which alters the position of the interface, changing the fractional amount of each chemistry in the particle.

When two immiscible fluids flow through a Y-junction, either droplet breakoff or coflow of the two streams can be observed, depending upon the flow rates used.^{30,34} We have chosen to operate in a regime where coflow is observed in order to make amphiphilic particles in a controllable fashion. Because the fluids used are immiscible, they coflow all the way to the exit of the microfluidic device. This leads to a segregation of the two phases all along the interface and is convenient for the formation of

(33) Decker, C.; Jenkins, A. D. *Macromolecules* **1985**, *18*, 1241–1244.

(34) Zhao, B.; Moore, J. S.; Beebe, D. J. *Science* **2001**, *291*, 1023–1026.

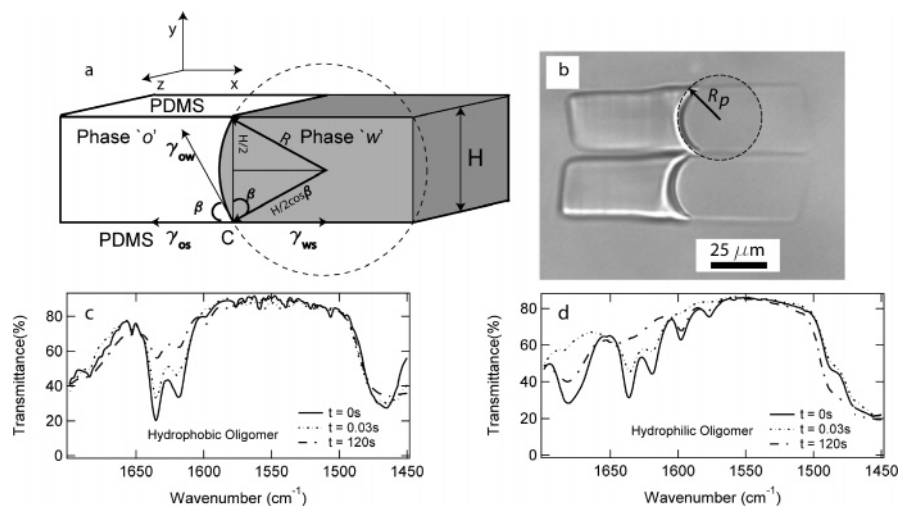


Figure 3. Characterization of particles. (a) A schematic showing the cross section of the microfluidic device. The x – y dimensions in Figure 1a are now visible. The interface between the hydrophilic and hydrophobic sections has a radius of curvature that is a function of the interfacial tensions between the two streams and the solid–liquid interfacial tension between the PDMS and the two streams. (b) A cross-sectional view of two particles lying on their sides. The curved interface between the hydrophilic and the hydrophobic portions depicted in (a) is clearly seen. The predicted radius of curvature of the interface, $R_p = 17.4 \mu\text{m}$, is overlaid on one of the particles as a guide to the eye. The measured radius of curvature using 10 particles is $R_m = 16 \mu\text{m} \pm 1.5 \mu\text{m}$. (c) FTIR data showing conversion of double bonds in the hydrophobic oligomer at $t = 0, 0.03$, and 120 s (fully cross-linked). At $t = 0.03$ s, 35% of all double bonds are converted. (d) FTIR data showing conversion of double bonds in the hydrophilic oligomer at $t = 0, 0.03$, and 120 s (fully cross-linked). At $t = 0.03$ s, 47% of all double bonds are converted.

large numbers of particles where diffusive mixing³⁵ might otherwise constrain the region available for polymerization. Channels with high aspect ratios (width/height $\gg 1$) are known to increase the operational phase space for the coflow of streams.³⁰ The channels we have used have aspect ratios ranging between 7 and 10, leading to stable flow rates with velocities as low as $100 \mu\text{m/s}$ for both phases. The particles shown in Figure 1b were formed using an exposure time of 0.03 s and a flow rate of $0.1 \mu\text{L/min}$ for both phases. A pause of 5 s was used between successive exposures.

A comprehensive analysis of particle monodispersity was performed by measuring the distribution of the five different length variables, w_1 , w_2 , w_3 , h_1 , and h_2 indicated in Figure 1b. In addition to the mask-defined edges of the particles (w_1 , w_3 and $(h_1 + h_2)$), the lengths of their hydrophilic (h_1) and hydrophobic (h_2) portions are dictated by the precise position of the interface when polymerization occurs. These lengths are all measured as the particles formed in the microfluidic device. Their distributions are shown in the histogram plots in Figure 1c–g. In all five dimensions that were measured, the coefficient of variation (COV) in size is less than 2.5% so that the particles can be classified as monodisperse.³⁶ Furthermore, by changing the length of the hydrophilic (h_1) and hydrophobic (h_2) sections, the extent of their amphiphilicity could also be tightly controlled. The thickness of the particles (y -direction in Figure 1b) is measured to be $25 \mu\text{m}$, which corresponds to a lubrication layer of thickness $2.5 \mu\text{m}$ at the top and bottom walls.¹³

The synthesized particles are allowed to collect in a reservoir, where they are pictured in Figure 2a,b. The particles shown are dispersed in ethanol in order to avoid clustering. As both the hydrophilic and hydrophobic polymeric precursors are completely soluble in ethanol, there is no preferential alignment of the

particles. As seen in the figure, the hydrophilic and hydrophobic sections of the particles are clearly distinguishable because of the difference in the refractive indices of the two sections. The hydrophilic section swells to a greater extent in ethanol, leading to a slight distortion in the original shape. The particles seen in Figure 2b are formed by inverting the mask so that the hydrophilic head is now smaller and the hydrophobic tail is the broader section. SEM images of individual particles from Figure 2a,b are seen in Figure 2c,d, respectively—their two distinct sections are again clearly visible. As seen in the images, when dry, the hydrophilic phase shrinks in comparison to the hydrophobic phase. To show that the method is general enough to synthesize different kinds of nonspherical particles with chemical anisotropy, we have also synthesized amphiphilic particles with a rodlike hydrophobic tail and a disk-shaped hydrophilic head (Figure 2e). Such a library of particles could be very useful when studying the effect of geometry and chemical anisotropy on mesoscale self-assembly⁴ and rheology.

As seen in Figure 2b, a cross-sectional (x – y plane in Figure 1a) view of these particles shows that the interface between the two sections has a finite curvature. This is caused by the immiscibility of the two flowing streams, leading to a sharp, curved interface (Figure 3b). As depicted in the schematic (Figure 3a), the hydrophobic (o) phase preferentially wets the PDMS over the hydrophilic (w) phase. The contact angle at the interface between the two phases and the PDMS wall, β , is dictated by the interfacial tension between the hydrophilic phase and the hydrophobic phase as well as by the solid–liquid interfacial tension between the PDMS and the two phases. When the imposed flow rates are changed, we observe that the widths of the streams are altered to minimize the pressure drop across the interface to a value that can be sustained by the equilibrium curvature of the interface. The interface is then observed to translate, but it then reaches an equilibrium state where its curvature and contact angle at the solid surface are not affected by the flow rates.³⁰ Since the interface formed is orthogonal to the direction of flow and does not move after reaching steady state, we believe that the interfacial properties measured for a stationary droplet can be used in the following analysis. Using simple geometry, we

(35) Stone, H. A.; Stroock, A. D.; Ajdari, A. *Annu. Rev. Fluid Mech.* **2004**, *36*, 381–411.

(36) Jilavenkatesa, A.; Dapkunas, S. J.; Lum, L.-S. H. *Particle Size Characterization*; Technical Report 960; National Institute of Standards and Technology; U.S. Government Printing Office: Washington, DC, 2001. According to the standards of the National Institute of Standards and Technology (NIST), a particle distribution can be considered monodisperse if at least 90% of the distribution lies within 5% of the median size.

predict the radius of curvature of the interface to be

$$R = \frac{H}{2 \cos \beta} \quad (1)$$

where H is the height of the channel. A simple force balance at the contact line (point C in Figure 3a) gives

$$\gamma_{ow} \cos \beta = \gamma_{ws} - \gamma_{os} \quad (2)$$

where γ_{ow} is the interfacial tension between phase o and phase w, and γ_{os} and γ_{ws} are the solid–liquid interfacial tensions between PDMS (s), and phases o and w, respectively. The right-hand side of eq 2 can be represented in terms of conveniently measurable properties like the contact angle of phase o and phase w on a PDMS surface surrounded by air and the surface tensions of phase o and phase w.

$$\gamma_{ws} = \gamma_{sa} - \gamma_{wa} \cos \theta_w \quad (3a)$$

$$\gamma_{os} = \gamma_{sa} - \gamma_{oa} \cos \theta_o \quad (3b)$$

where γ_{sa} is the surface tension of a native PDMS surface, γ_{oa} and γ_{wa} are the surface tensions of phases o and w, respectively. θ_o and θ_w are the contact angles of phases o and w on a native PDMS surface, respectively. Subtracting eq 3b from 3a, we eliminate γ_{sa} to get

$$\gamma_{ws} - \gamma_{os} = \gamma_{oa} \cos \theta_o - \gamma_{wa} \cos \theta_w \quad (4)$$

Using eqs 1, 2, and 4, we now have

$$R = \frac{H\gamma_{ow}}{2(\gamma_{oa} \cos \theta_o - \gamma_{wa} \cos \theta_w)} \quad (5)$$

Using experimentally measured values of γ_{ow} (7.35 ± 0.12 mN/m), γ_{wa} (40.49 ± 0.24 mN/m), γ_{oa} (32.59 ± 0.26 mN/m), θ_o (51°), and θ_w (69.5°), and using $H = 30 \mu\text{m}$, we predict $R = 17.4 \mu\text{m}$ (Figure 3b). This matches well with the experimentally determined value of $16 \pm 1.5 \mu\text{m}$. The interfacial properties of the streams can therefore be used to tune the curvature of the interface between the two sections. We also see that the radius of curvature of the interface is proportional to the channel height.

The extent of cross-linking of the particles in the two different phases was characterized by measuring the percentage of double bonds converted using FTIR spectroscopy (Figure 3c,d). All particles in this study are made using 0.03 s of exposure to UV light. In this time, the conversion of double bonds was found to be 47% in the hydrophilic phase and 35% in the hydrophobic phase.

Since the conversion of double bonds required to cross-link multifunctional acrylates successfully is typically less than 5%,³⁷ we conclude that the exposure dose received is sufficient to cross-link the particles.

Like amphiphilic molecules, particles possessing both hydrophilic and hydrophobic sections exhibit a tendency to orient themselves in order to minimize their surface energy.^{19,20} While thermal energy alone is insufficient to enable these particles to explore their energy landscape, providing external energy through agitation helps these particles find their energy minima and self-assemble. In a series of experiments, we isolated the amphiphilic particles that we formed and induced them, using agitation, to assemble either in a pure aqueous phase or at the interface of w/o or o/w emulsions. The results show that the particles have a

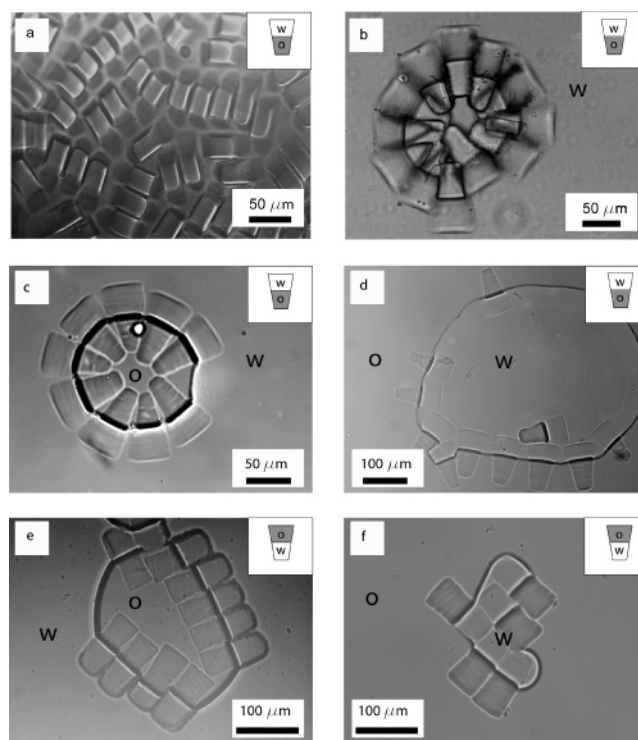


Figure 4. Self-assembled structures formed using biphasic hydrophilic-hydrophobic particles. In (a)–(f), the cartoon in the inset shows an individual particle with its hydrophilic portion labeled w and its hydrophobic portion labeled o. (a) Particles with a large hydrophilic head and a small hydrophobic tail cluster in a bath of TMPTA. Their hydrophobic tails are all uniformly pointed out of the page, while their hydrophilic heads point into the page. (b) Particles seen in (a) form a micelle-like structure in water. The geometry of the particles enables them to form a circular structure to shield the inner hydrophobic sections. (c,d) Particles with a large hydrophilic head and a small hydrophobic tail assemble at the interface of an oil-in-water and a water-in-oil emulsion, respectively. The hydrophilic section preferentially stays in the water, while the hydrophobic section stays in the oil. (e,f) Particles with a small hydrophilic head and a large hydrophobic tail at the interface of an oil-in-water and a water-in-oil emulsion, respectively. The hydrophilic head swells in water, leading to deformation of the particles from their original shape.

strong tendency to orient themselves in order to minimize their surface energy. In the upper right corner of each picture in Figure 4, we have drawn cartoons of the particle to clarify what particles have been used in each experiment. In these cartoons, the symbol w refers to the hydrophilic section of the particles and o to their hydrophobic sections. Particle assembly was restricted to two dimensions by performing experiments in a film of fluid that is sandwiched in between two PDMS-coated glass slides.

We first looked at particles in a single external phase. Even when clustered in the reservoir in a phase containing only monomer, the particles showed a tendency to keep their like sections close to each other (Figure 4a). As seen, all the particles have their hydrophilic heads pointing into the page and their hydrophobic tails pointing out of the page. Further, when the particles with a large hydrophilic head and a smaller hydrophobic tail were agitated, they clustered to form micelle-like structures (Figure 4b) when dispersed in water. As seen in the figure, the particles form a closed structure in order to shield the hydrophobic tails from the external aqueous phase. The tapering wedge-shaped geometry of the particles induced the curvature of the micelles.

We also found that, when a particle-loaded two-phase system containing water and toluene is agitated to form emulsion droplets, the particles preferentially migrated to the interface between the

two phases as expected.^{3,6,11,38} Such particles are strongly adsorbed at interfaces because of the energetic gains caused by both the decrease in o/w interfacial area and the partitioning of the solid phases into the preferred liquid phase (PEG-DA in water and TMPTA in toluene). Particles with a large hydrophilic head and a small hydrophobic tail orient themselves at the interface of an oil-in-water emulsion such that the entire hydrophilic portion is in the water while the hydrophobic section is confined to the oil (Figure 4c). The interface between oil and water is clearly seen where there is a gap between particles. When the same particles are introduced into a two-phase system that is prone to forming water-in-oil type emulsions, the particles now change their orientation so that their hydrophobic tails are in the oil while their hydrophilic heads are confined to the water droplet (Figure 4d). Particles with a small hydrophilic head and a large hydrophobic tail assemble at the interface of o/w or w/o emulsions such that their surface energy was minimized (Figure 4e,f). The particles also deform the emulsion droplets in order for the interface between the two particle sections to coincide with the emulsion droplet interface (Figure 4d,f)

4. Conclusion

We have presented a new, microfluidic method that allows for the synthesis of generic 2-D extruded shapes that also contain spatially segregated chemical functionality. By polymerizing across laminar coflowing streams containing different chemistries, we have shown the synthesis of particles bearing both hydrophilic and hydrophobic chemistries. Using flowing streams of polymer in a microfluidic device, we are able to provide much higher particle throughput than polymerization performed across static fluids. Also, by using a fluid–fluid interface that is parallel to the path of propagation of light, we are able to make different sections of the particle such that they bear different geometries. The method is equally applicable to synthesizing particles containing magnetic, pH-responsive, or other kinds of chemistries.

Particle shape may be conveniently defined using a mask, and the extent of each chemistry can be tuned simply by moving the microscope stage or by altering the widths of the streams (when more than two streams are present). This method possesses the unique advantage of being able to generate particles containing more than two chemistries in any extruded 2-D shape. For example, we can go beyond the Janus o–w motif presented here and create o–w–o bar-shaped particles. The interface between the independent sections of the particles may be tuned by changing the surface properties of the streams, while the mechanical properties of the particles can be altered by varying exposure time and hence cross-linking density. The length scale of the particles synthesized in this study is on the order of 100 μm , but we believe that such amphiphilic particles can easily be made down to lengths of 10 μm . However, further adjustments to the technique will be required to synthesize colloidal, amphiphilic particles because of the finite curvature of the interface.

Furthermore, we have demonstrated that the chemical anisotropy of the particles may be used to aggregate the particles into structures reminiscent of their molecular analogs. This method can enable the synthesis of particles that are synthetic in design or inspired by nature (like surfactants). The particles can then serve as “coded” building blocks that assemble to build superstructures useful both for fundamental studies and in the synthesis of new materials and devices. The method would be extremely useful to test the effect of particle geometry and chemical anisotropy on self-assembly at the micron scale. Bar-coded particles³⁹ with multiple chemistries may also find applications in diagnostics and medicine where the detection of multiple analyte species simultaneously is of great importance.

Acknowledgment. We gratefully acknowledge the support of NSF NIRT grant no. CTS-0304128 for this project. We thank Patrick Underhill for useful discussions.

LA062512I

(38) Binks, B. P. *Curr. Opin. Colloid Interface Sci.* **2002**, 7, 21–41.

(39) Finkel, N. H.; Lou, X.; Wang, C.; He, L. *Anal. Chem.* **2004**, 76, 352A–359A.